ePESSTO+ (advanced Public ESO Spectroscopic Survey of Transient Objects*) SSDR1*

Abstract

ePESSTO+ (advanced Public ESO Spectroscopic Survey of Transient Objects – ESO program IDs 1103.D-0328 and 106.216C) started in April 2019 and it is currently ongoing at the New Technology Telescope using the instruments EFOSC2 and SOFI. It is the second extension of the PESSTO survey (PI: Smartt). We typically targeted supernovae and optical transients brighter than 20 mag for classification and selected science targets for detailed follow-up. We used standard EFOSC2 setups providing spectra with resolutions of 13-17Å between 3680-10320Å. A subset of the brighter science targets was selected for SOFI spectroscopy with the blue and red (rarely) grisms (resolutions 23Å - 33Å) and imaging with broadband JHKs filters. In the following, we define SSDR1 as the set of data products from April 2019 to October 2021, covering the first 2.5 years of ePESSTO+ operations[1]. This release includes the EFOSC2 and SOFI spectra, as well as reduced SOFI images all obtained during the first 2.5 years of operations.

Overview of Observations

ePESSTO+ was allocated 90-100 nights per year, in visitor mode (and during the pandemic in deputy visitor mode), on the ESO NTT. There were no observations planned during the months the Galactic centre is at optimal right ascension which make it difficult to search for extragalactic SNe and there is also large time pressure from the ESO community for Milky Way stellar science. ePESSTO+ was typically allocated 10 nights per month split into three sub-runs of 4N, 3N and 3N. Typically the middle sub-run is dark time, while the two others are grey/bright with the moon up for around 50% of the time. The instruments are EFOSC2 and SOFI and both spectroscopy and imaging modes are employed. The ePESSTO+ collaboration host public webpages with useful information in the form of night reports, observing conditions, observing with the NTT, and the data reduction pipeline. This information is updated during the survey and users should read this document with the information on www.pessto.org and the wiki pages that the homepage points to. A summary of the spectroscopic data setups is given in Tables 1 and 2. The science target selection strategy is described in detail in Smartt et al. (2015).

Table 1. *ePESSTO+ settings for EFOSC2 spectroscopy. The blocking filter OG530 is used only (and always) for Gr#16. The GG495 blocking filter is occasionally used for Gr#20. The 1" slit projects to 3.5 binned pixels. The column headed Arclines indicates the number of lines used. The RMS is the typical residual for the wavelength calibration solution.*

Grism	Wavelength (Å)	Filter (blocking)	Dispersion (Å / pix)	Resolution (Å - 1" slit)	Arclines (number)	RMS (Å)
#13	3650 – 9250	None	5.5	18.2	13 – 15	0.10 – 0.15
#11	3345 – 7470	None	4.1	13.8	9	0.10 – 0.15
#16	6000 – 9995	OG530	4.2	13.4	11 – 14	0.05 – 0.10
#18	4700 – 6770	None	1.0	7.6	7	0.01 – 0.08
#20	6047 – 7147	GG495	0.55	2.0	12	0.05 – 0.07

Table 2*. ePESSTO+ settings for SOFI spectroscopy. The 1" slit projects to 3.4 pixels FWHM, measured from arc lines. The column headed Arclines indicates the number of lines used. The RMS is the typical*

[1] Note that there are no observations for roughly 7 months in 2020 due to the onset of the covid-19 pandemic.

residual for the wavelength calibration solution. The order blocking filters used are 0.925μm (GBF) and 1.424μm (GRF) "cut on" filters.

Grism	Wavelength (μm)	Filter (blocking)	Dispersion (Å / pix)	Resolution (Å - 1" slit)	Arclines (number)	RMS (Å)
Blue	0.935 – 1.654	GBF	6.95	23	12 14	0.1 – 0.2
Red	1.497 – 2.536	GRF	10.2	33	7 - 8	0.2 – 0.5

Release Content

ePESSTO+ observes single targets in long-slit mode and selects targets for two purposes as described in Smartt et al. (2015). The first is to classify targets as early as possible after discovery. ePESSTO+ takes targets from many different public surveys which report their discoveries of transient sources. These "classification" spectra are taken with Grism#13 (and seldomly with Grism#11) and typically we aim for signal-to-noise in the continuum between 10-20 depending on the magnitude of the source. The main purpose is to reliably screen targets to determine their classification and redshift. The scientific goal of ePESSTO+ is the same as PESSTO (Smartt et al. 2015). Hence a detailed follow-up and time series spectroscopic monitoring of supernovae at the extremes of the known population e.g. the most luminous, the faintest, the fast declining etc. Hence the screening classification spectra are necessarily kept short to minimize the time observing normal supernovae and maximize the time available for scientific follow-up. In 2.5 years, ePESSTO+ has taken spectra of 2138 objects. From this list, 154 supernovae (25 of which are super-luminous supernovae and 2 Icn a new type of rare interacting transient), 1 supernova imposter, 15 tidal disruption events, 2 LBV, 2 AGN, 4 supernovae light echoes were picked as interesting science targets and these were scheduled for follow-up time series EFOSC2 optical spectroscopy, with the brightest also having SOFI spectra. A summary of these 178 ePESSTO+ Key Science targets and the spectral data sets taken is given in Table 3. The total numbers of spectra released for these 178 "ePESSTO+ Key Science" targets are 1117 EFOSC2 spectra and 17 SOFI spectra. The EFOSC2 number includes any transient classification spectra taken. ePESSTO+ has used EFOSC2 in imaging mode to take acquisition images of many of the targets before a spectrum is taken and, in some cases, multi-colour photometry is taken. Smartt et al. (2015) describes the rationale for lightcurve construction for PESSTO (and hence ePESSTO+) science targets, which are typically bright enough to be done with smaller aperture facilities. SOFI near infra-red spectra are nearly always taken when SOFI imaging is taken. The higher resolution EFOSC grisms Gr#18 and Gr#20 were employed occasionally to allow higher spectral resolution for objects with H-Balmer lines in emission (see Table 1 for details of resolutions). In total, the SSDR1 contains 13.74 GB of data and the numbers of images and spectra are given in Table 4. In total there are 2138 EFOSC2 spectra released. These include the 1117 EFOSC2 spectra of Table 3. The remaining 1021 EFOSC spectra relate to objects for which we took spectra but did not pursue a detailed follow-up campaign. There are more spectra than objects simply due to the fact that in some cases ePESSTO+ took more than one spectrum for classification due to either low signal-to-noise in the first spectrum, or ambiguous classifications that needed further spectra to allow a secure analysis. Generally, the first spectrum taken of an object was enough for a classification. However, there were circumstances in which further spectra were needed due to either low signal-to-noise, or a real ambiguity. The most common cause of ambiguity in classification are objects showing featureless blue continua. These are usually young type II SNe, but can be Galactic CVs, tidal disruption candidates, or moderate redshift superluminous supernovae. In these cases, further spectra usually show spectral features to allow redshift and classifications. The classifications released by ePESSTO+ are based on the set of early spectra taken. ePESSTO+ has taken EFOSC2 images which include multi-colour follow-up images of science targets, EFOSC2 acquisition images, and at times standard star fields (fields are defined in Smartt et al. 2015). These EFOSC2 images will be astrometrically and photometrically calibrated (as far as the small field of view of EFOSC2 will allow). The raw images are available in the ESO archive. In some cases, the astrometric position of the science target on SOFI (or the EFOSC2) images can be of order 0.5 – 1.5 arcsec different to that recorded in the headers of the 1D spectral files. The coordinates in the 1D spectral files are those of the target and these are taken from a range of surveys which can have minor, but measurable, errors in the absolute astrometry. When we observed the transient host galaxy at the same exact position as the transient to gather information on the local environment, the OBJECT keyword will have the galaxy name rather than the

transient, e.g. OBJECT = '2MASS J11470402+1933032' for the host galaxy of SN2018atq. The coordinates in the SOFI and EFOSC2 images are likely to be as good if not better than those originally provided from the feeder surveys, but discrepancies are typically less than 1.5 arcseconds.

***Table 3**. ePESSTO+ SSDR1 Key Science targets. These targets were selected for detailed follow-up in the 2.5 years of survey operations, initially with EFOSC2 and with SOFI when possible. The numbers refer to the numbers of epochs of spectra taken with each grism. Gr11, Gr13, Gr16, Gr18 and Gr20 refer to the EFOSC2 grisms and GB, GR refers to the SOFI grism (GB = blue, GR = red, with details in Table 2).*

Target	Type	Number of Spectra	Comments
AT2017gge	TDE	1xGr13, 1xGr18, 1xGB	Onori et al. 2022
AT2018dyb	TDE	3xGr11, 1xGr16	Leloudas et al. 2020
AT2018fyk	TDE	2xGr11	Charalampopoulos et al. 2022
AT2018hla	AGN	1xGr11	
AT2018hyz	TDE	8xGr11	Short et al. 2020
AT2018lna	TDE	4xGr13	Charalampopoulos et al. 2022
AT2018lqi	SLSN-II	4xGr13	
AT2019ahk	TDE	7xGr11, 5xGr16, 1xGB	
AT2019dsg	TDE	7xGr13	Cannizzaro et al. 2021
AT2019hdl	TDE	1xGr11, 10xGr13, 1xGr16	
AT2019lwu	TDE	4xGr11, 6xGr13	
AT2019pev	TDE	4xGr11, 4xGr16	
AT2019qiz	TDE	24xGr11, 2xGr13, 7xGr16	Nicholl et al. 2020
AT2019udc	LBV	1xGr11, 1xGr13, 1xGr16	Valerin et al. submitted
AT2019wbg	LBV	7xGr11, 4xGr13, 2xGr16	
AT2019wxt	SN IIb	5xGr13	
AT2019xis	Light echo	1xGr11, 6xGr13	
AT2020vwl	TDE	2xGr11, 4xGr13	
AT2020xys	AGN	9xGr11, 9xGr16	
AT2020zso	TDE	4xGr11, 2xGr13, 1xGr16	Wevers et al. 2022
AT2021blz	TDE	18xGr13	
AT2021jjm	TDE	4xGr13	
OGLE19wcj	SN Ia	2xGr11, 1xGr13, 1xGr16	
SDSSJ0938+1353	Light echo	1xGr11, 1xGr16	
SDSSJ1342+0530	Light echo	1xGr11, 1xGr16	
SDSSJ1350+2916	Light echo	2xGr11, 2xGr16	
SN2016ezh	SN II	4xGr11, 5xGr16, 1xGr20	
SN2017ens	SLSN-I	2xGr11, 2xGr16	Chen et al. 2018
SN2017hcc	SN IIn	1xGr11, 1xGr16	Moran et al. 2023
SN2017ivv	SN II	3xGr13	Gutierrez et al. 2020
SN2018atq	SNSL II	1xGr11, 1xGr13, 1xGr16	
SN2018evt	SN Ia	4xGr13	Wang L. et al. 2022 submitted
SN2018giu	SN Ic-BL	3xGr13	

SN2018ibb	SLSN-I	4xGr13	Schulze et al. in prep.
SN2019bao	SN II-pec	2xGr11	
SN2019asz	SN II	4xGr13	
SN2019axz	SN II	2xGr13	
SN2019bdz	SN Ia	3xGr13	
SN2019bka	SN Ia-91T-like	5xGr13	
SN2019but	SN Ibn	2xGr11, 4xGr16	
SN2019bwa	SN Ib-pec	4xGr13	
SN2019bwb	SN IIn	2xGr13	
SN2019cqc	SLSN-II	2xGr11, 12xGr13, 4xGr16	
SN2019cri	SN Ic	1xGr11, 4xGr13, 1xGr16	Prentice et al. 2021
SN2019cwt	SN Ic-pec	4xGr13	
SN2019cxt	SN I	7xGr13	
SN2019cxx	SN Ia	1xGr13, 1xGB	
SN2019dke	SN II	3xGr13	
SN2019dts	SN II	2xGr13	
SN2019ecx	SN Ia-91bg-like	2xGr11, 2xGr16	
SN2019enz	SLSN-I	2xGr11, 1xGr13, 2xGr16	
SN2019esa	SN IIn	4xGr11, 3xGr13, 8xGr16, 2xGr18, 2xGr20, 4xGB	
SN2019fcg	SN Ia-CSM	6xGr13	
SN2019fcn	SN II	4xGr13	
SN2019fdr	SLSN-II	1xGr11, 2xGr13, 1xGr16	
SN2019fht	SN II	2xGr13	
SN2019fmr	SN Ia-91T-like	4xGr13	
SN2019gaf	SN IIb	2xGr11, 2xGr13, 2xGr16	
SN2019gbx	SN Ia	1xGr11, 1xGr13, 1xGr16	
SN2019gfm	SN Ic-BL	4xGr13	
SN2019gqi	SLSN-I	2xGr13	
SN2019hcc	SLSN-I	1xGr11, 8xGr13	Parrag et al. 2021
SN2019hge	SN IIb	2xGr11, 4xGr13, 4xGr16	Prentice et al. 2021
SN2019jyn	SN Ic	2xGr11, 3xGr13, 3xGr16	
SN2019kcy	SLSN-I	4xGr11, 1xGr16	
SN2019ltw	SN II	3xGr11, 2xGr13, 3xGr16	
SN2019mry	SN IIn-pec	1xGr11, 2xGr13, 1xGr16, 1xGr20	
SN2019mrz	SN II	8xGr13	
SN2019muj	SN Iax[02cx-like]	3xGr11, 3xGr13, 3xGr16	Barnabas et al. 2021
SN2019nhs	SLSN-I	4xGr13	
SN2019odp	SN Ic-BL	6xGr11, 6xGr16	
SN2019ofc	SN II	6xGr13	
SN2019pcr	SN II	2xGr11, 5xGr13, 1xGr16	
SN2019pnl	SN II	3xGr13	
SN2019qem	SN IIn	16xGr11, 2xGr13, 16xGr16	

SN2019rwd	SN II	2xGr11, 6xGr13, 2xGr16	
SN2019sox	SN II	2xGr13	
SN2019spa	SN Ia	2xGr11, 1xGr13, 2xGr16	
SN2019ssi	SN II	3xGr13	
SN2019szu	SLSN-I	7xGr13, 1xGr16	
SN2019tpl	SN IIn	2xGr11, 1xGr13, 2xGr16	
SN2019tsf	SN Ib	2xGr13	
SN2019tuq	SN II	4xGr13	
SN2019uhm	SN II	5xGr13	
SN2019unb	SN II	4xGr11, 10xGr13, 4xGr16	Prentice et al. 2021
SN2019vjl	SN II	4xGr13	
SN2019vqd	SN II	16xGr11, 2xGr13, 13xGr16	
SN2019vrq	SN Ia-91T-like	3xGr11, 1xGr13, 3xGr16	
SN2019yvr	SN Ib	1xGr11, 5xGr13, 1xGr16	
SN2019zcr	SLSN-II	2xGr11, 1xGr13, 2xGr16	
SN2020aatb	SN II	4xGr13	
SN2020abjx	SLSN-I	1xGr11, 1xGr16	
SN2020abtf	SN II	3xGr11, 10xGr13, 3xGr16	
SN2020abyj	SN II	3xGr13	
SN2020acat	SN IIb	18xGr11, 17xGr16, 1xGB	Medler et al. 2022
SN2020acbm	SN II	3xGr13	
SN2020ad	SN II	2xGr13	
SN2020adow	SN Ic-BL	8xGr11, 8xGr16	
SN2020aer	SN II	3xGr13	
SN2020ank	SLSN-I	2xGr11, 2xGr13, 3xGr16	
SN2020aqe	SN II	2xGr13	
SN2020aze	SN II	4xGr13, 1xGB	
SN2020bfb	SN Ic	3xGr13	
SN2020bij	SN II	2xGr13	
SN2020bkp	SN II	3xGr13	
SN2020cpg	SN Ib	4xGr11, 1xGr13, 5xGr16	Medler et al. 2021
SN2020cui	SN IIn	1xGr11, 1xGr13, 1xGr16, 1xGB	
SN2020cwd	SN Ibn	3xGr11, 1xGr13, 4xGr16	
SN2020dfh	SN IIn	4xGr13	
SN2020dko	SN Ia	2xGr11, 1xGr13, 3xGr16	
SN2020ejm	SN Ia	3xGr11, 3xGr16	
SN2020llx	SN II	3xGr13	
SN2020ocz	SN II	9xGr13	
SN2020oi	SN Ic	3xGr11, 3xGr16, 1xGB	
SN2020pvb	SN IIn	6xGr11, 6xGr16	Elias-Rosa et al. sub-mitted

SN2020skx	SN II	2xGr13	
SN2020ue	SN Ia	6xGr11, 2xGr13, 5xGr16, 2xGB	
SN2020uew	SLSN-I	2xGr11, 14xGr13	
SN2020uik	SN II	4xGr13, 1xGr16	Irani et al. 2022
SN2020usa	SLSN-II	3xGr13	
SN2020utf	SN II	2xGr13	
SN2020uwl	SN II	1xGr11, 2xGr13, 1xGr16	
SN2020vef	SN II	1xGr11, 5xGr13	
SN2020voh	SN II	4xGr13	
SN2020vzv	SN II	2xGr11	
SN2020xga	SLSN-I	2xGr11, 5xGr13, 1xGr16	
SN2020xkw	SN II	8xGr13	
SN2020xoq	SN II	2xGr13	
SN2020yex	SN Ia	2xGr13	
SN2020ykb	SN II	2xGr13	
SN2020yzo	SN II	6xGr13	
SN2020zbf	SLSN-I	1xGr11, 6xGr13, 1xGr16	
SN2020zgl	SN Ib-pec	2xGr11, 1xGr13, 2xGr16	
SN2020znl	SN II	5xGr11, 4xGr13	
SN2020znr	SLSN-I	12xGr11, 2xGr13, 11xGr16	
SN2021aek	SN II	7xGr11, 1xGr16	
SN2021bnw	SLSN-I	6xGr11, 1xGr13, 5xGr16	
SN2021can	SN II	3xGr11	
SN2021cgu	SN II	2xGr13	
SN2021ckj	SN Icn	3xGr13	Nagao et al. 2023
SN2021csp	SN Icn	2xGr11, 10xGr13, 2xGr16	
SN2021dbg	SN II	2xGr11	
SN2021ddc	SN	4xGr13	
SN2021dn	SN Ia	4xGr11, 4xGr16	
SN2021dov	SN Ia	5xGr11, 1xGr13, 6xGr16	
SN2021een	SLSN-I	3xGr13	
SN2021ek	SLSN-I	3xGr13	
SN2021fmu	SLSN-II	1xGr11, 3xGr13, 1xGr16	
SN2021foa	SN IIn	3xGr11, 3xGr16	
SN2021fox	SN II	4xGr13	
SN2021fpl	SLSN-I	1xGr11, 1xGr16	
SN2021fxf	SN Ic	3xGr11, 1xGr13, 3xGr16	
SN2021fxy	SN Ia	4xGr11, 3xGr13, 4xGr16	
SN2021gno	SN II	1xGr11, 2xGr13, 1xGr16	
SN2021gvm	SN II	2xGr13	
SN2021hiz	SN Ia	2xGr11, 2xGr16	
SN2021hku	SN Ic-BL	1xGr11, 1xGr16	
SN2021iso	SN II	5xGr11, 1xGr13, 1xGr16	

SN2021jbi	SN IIn	6xGr13	
SN2021kgj	SN IIn	1xGr11, 2xGr13, 1xGr16	
SN2021ok	SN II	2xGr13	
SN2021pc	SN Ia	2xGr11, 1xGr13, 2xGr16	
SN2021qqu	SN II	4xGr13	
SN2021qvr	SN II	2xGr13	
SN2021qvw	Impostor-SN	3xGr11, 1xGr13, 6xGr16	
SN2021tiq	SN II	2xGr13	
SN2021tyw	SN II	8xGr11, 8xGr16	
SN2021uds	SN IIn-pec	6xGr11, 1xGr13, 6xGr16, 2xGB	
SN2021uhk	SN Ib-pec	4xGr11, 2xGr16	
SN2021uqw	SN II	2xGr11, 1xGr13	
SN2021uvy	SN Ib/c	4xGr11, 4xGr16	
SN2021vtk	SN Ib	2xGr11, 3xGr16	
SN2021vtq	SN Ia	1xGr11, 1xGr16	
SN2021vyj	SLSN-II	1xGr11	
SN2021wvd	SN II	1xGr11, 1xGr13, 2xGr16	
SN2021ybc	SN IIb	2xGr11, 3xGr16	
SN2021yja	SN II	2xGr11, 2xGr16, 1xGB, 1xGR	Hosseinzadeh et al. 2022
SN2021zj	SN II	7xGr11, 1xGr16	

Table 4. *The total number of science files released in the various formats is described here.*

File Type	Format	Number of Files	Data Volume
EFOSC2 1D spectra	Binary table	2157	101.19 MB
EFOSC2 2D spectral images	FITS image	2157	6.92 GB
SOFI 1D spectra	Binary table	18	860.62 KB
SOFI 2D spectral images	FITS image	18	57.89 MB
SOFI images	FITS image	480	3.39 GB
SOFI image weights	FITS image	480	3.39 GB
TOTAL		5310	13.85 GB

Release Notes

Data Reduction, Calibration, Data Quality and Known Issues

1. EFOSC 2 Optical spectroscopy

Bias calibration: a set of 11 bias frames is typically taken each afternoon of ePESSTO+ EFOSC2 observations and is used to create a nightly master bias. This nightly master bias frame is applied to all EFOSC2 data taken, including the spectroscopic frames, the acquisition images and any photometric imaging. The frame used for the bias subtraction can be tracked in the header keyword.

ZEROCOR = 'bias_20130402_Gr11_Free_56448.fits

The file name gives the date the bias frames were taken, the Grism and filter combinations for which it is applicable (of course for biases this is not relevant but the pipeline keeps track with this nomenclature) and the MJD of when the master bias was created. The dark current is less than 3.5 e^{-} pix^{-1} hr^{-1}, hence with typical ePESSTO+ exposures being 600-1800s, no dark frame correction is made.

Flat field calibration: the ePESSTO+ survey takes sets of spectroscopic flatfields in the afternoons at a typical frequency of once per sub-run of 3-4 nights. Five exposures are taken with maximum count levels of 40,000-50,000 ADU for each of the grism, order sorting filter, and slit width combinations that we use (8 combinations in total). Each of these is combined to give a masterflat which can be associated with the appropriate science observations from the sub-run.

FLATCOR = 'nflat_20130413_Gr11_Free_slit1.0_100325221_56448.fits'

The EFOSC2 CCD#40 is a thinned chip, hence has significant fringing beyond 7200Å and the severity depends upon the grating used. The only way to remove fringing (in spectroscopic mode) is to take a calibration flat field lamp exposure immediately after or before the science image and use this to divide into the science spectrum. ePESSTO+ always takes internal lamp flats (3 exposures of typically 40,000 ADU maximum count level) after taking any science spectra with Gr#16. More details on the exact methods used are given in Smartt et al. (2015).

Cosmic ray removal: the PESSTO pipeline (ePESSTO+ uses the same pipeline as PESSTO as EFOSC2 and SOFI set up did not change since the beginning of PESSTO) incorporates a modified version of the python implementation of LaCOSMIC (Van Dokkum 2001) to remove cosmic rays in the central 200 pixels around the object (i.e. central pixel ±100 pixels).

Arc frames and wavelength calibrations: arc frames are taken in the evening before observing and in the morning after the night finishes. EFOSC2 has helium and argon lamps and ePESSTO+ uses both of these lamps turned on together. No arc frames 20 are taken during the night to reduce overheads. Although EFOSC2 suffers from significant flexure as the instrument rotates at the nasmyth focus (which can be 4 pixels over 200 degrees in rotation), the flexure causes a rigid shift of the wavelength frame. Hence, we apply the calibration determined from the evening arc frames and adjust this with a linear offset as measured from either the skylines or atmospheric absorption lines. Relatively high order Legendre polynomial fits (5- 6) are needed to fit the EFOSC2 arc lines with a fit which produces no systematic residuals. The number of arc lines used for the dispersion solution of each object, along with the RMS error, is given in the header of the reduced spectra by the keywords LAMNLIN and LAMRMS respectively. The formal RMS values are probably too small to realistically represent the uncertainty in the wavelength calibration at any particular point, given the FWHM of the arclines is 13-17Å. Hence this might suggest over-fitting of the sampled points. As a comparison, Legendre polynomials with order 4 produced obvious systematic residuals and RMS values of between 0.4-1.0 Å for a 1.0" slit and 1-1.8 Å for a 1.''5 slit. For exposures longer than 300 s, the linear shift applied to the dispersion solution is measured from the night sky emission lines. For shorter exposures such as spectrophotometric standards, the night sky lines are not visible, and the shift is instead measured from the telluric absorptions in the extracted 1D spectrum. The linear shifts are typically in the range of 6-13 Å for Gr#11 and Gr#13. In the case of Gr#16 spectra the shifts were usually smaller, usually 4-9 Å. This value of linear shift is recorded in the header keyword SHIFT. The linear shifts are calculated by cross-correlating the observed spectrum (sky or standard) with a series of library restframe spectra which are offset by 0.1 Å. The library spectrum which produces the minimum in the cross correlation function is taken as the correct match and this shift is applied. This method limits the precision of the shift to 0.1 Å, which is roughly 1/40 of a pixel and less than 1/100 of a resolution element. This value of 0.1 Å is recorded in the header as the systematic error in the wavelength calibration (SPEC_SYE). For all EFOSC2 spectra the wavelength axis reports wavelengths as measured in dry air.

Spectrophotometric standards and flux calibration: ePESSTO+ uses a set of 9 spectrophotometric standard stars (see Smartt et al. 2015) and we typically observe an EFOSC2 spectrophotometric standard three times per night (start, middle and end), although if there are significant SOFI observations or weather intervenes then this may be reduced. Generally, the three observations will include 2 different stars and a set of observations is taken with all grism, slit and filter

combinations used during the nights observation. To remove any second-order contamination in the flux standards, ePESSTO+ always takes Gr#13 data for these stars with and without the filter GG495, to allow correction for the effect during pipeline reductions. Flux standards are always observed unless clouds, wind or humidity force unexpected dome closure. Hence even during nights which are not photometric, flux standards are taken and the spectra are flux calibrated; we deal with the issue of the absolute flux reliability below. A sensitivity function is derived for each EFOSC2 configuration from the spectrophotometric standards observed for each night. This was then applied to the final reduced spectra. In a few instances, a sensitivity curve was not created for a particular configuration on a given night, as there were no appropriate standards observed. In these cases, the sensitivity function from the preceding or following night was used. The standard method of ensuring spectra are properly flux calibrated is to compare synthetic photometry of the science spectra with contemporaneous calibrated photometry and apply either a constant, linear or quadratic multiplicative function to the spectra to bring the synthetic spectra into line with the photometry. For ePESSTO+ SSDR1 this is not yet possible for all spectra since the photometric lightcurves are not yet finalised for many of the science targets and the classification spectra do not have a photometric sequence. However, it is useful to know what the typical uncertainty is in any flux calibrated ePESSTO+ spectrum, and this is encoded in the header keyword FLUXERR. ePESSTO+ observes through non-photometric nights, and during these nights all targets are still flux calibrated. Hence the uncertainties in flux calibrations come from transparency (clouds), seeing variations that cause mismatches between sensitivity curves derived using standards with different image quality, and target slit positioning. Finally, photometric flux is generally measured with point-spread-function fitting which inherently includes an aperture correction to determine the total flux whereas spectroscopic flux is typically extracted down to 10 per cent of the peak flux (a standard practice in IRAF's apall task). All of this means that large percentage variations are expected, and we carried out tests as to how well this method works and what is the reliability of the absolute flux calibration in the spectra. In Smartt et al. (2015) we describe these quantitative tests. We find that the RMS scatter in the absolute spectroscopic flux calibration is 36% and this is recorded in the headers of all spectra.

FLUXERR = 36 /Fractional uncertainty of the flux [%]

Science users should use this as a typical guide, if the seeing (as can be measured on the 2D frames and acquisition images) and night conditions (from the PESSTO wiki night reports; see Smartt et al. 2015) are reasonable.

Telluric absorption correction: ePESSTO+ uses a model of the atmospheric absorption to correct for the H2O and O2 absorption (see Smartt et al. 2015 for details). This is carried out for all grism setups. The intensities of H2O and O2 absorptions in the atmospheric absorption model are first Gaussian smoothed to the nominal resolution of each instrumental setup, and then rebinned to the appropriate pixel dispersion. The pipeline then scales the model spectrum so that the intensities of H2O and O2 absorptions match those observed in the spectrophotometric standards, hence creating multiple model telluric spectra per night. Each science spectrum is than corrected for telluric absorption, by dividing it by the smoothed, re-xbinned, and scaled absorption model which is most closely matched in time i.e. closest match between the standard star observation time and the science observation time.

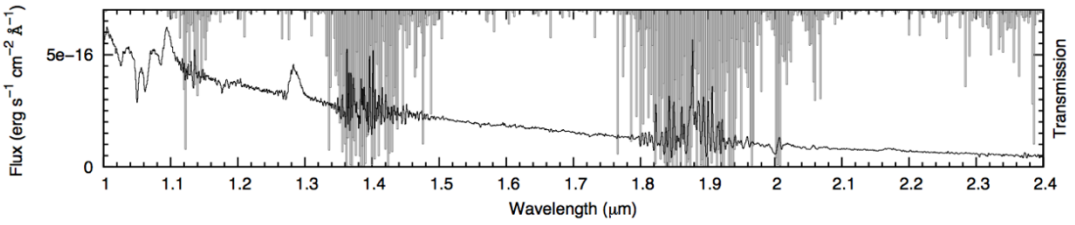

Figure 1. *Combined blue and red grism SOFI spectra of SN 2012ec taken on 2013 September 24 (under the previous survey PESSTO). Overplotted in grey is the atmospheric transmission, showing the correspondence between regions of low transparency and poor S/N in the spectrum.*

2. SOFI Near Infrared spectroscopy

Similar to ePESSTO+ observations and reductions for EFOSC2, we aim to homogenise the SOFI observations and calibrations and tie them directly to what is required in the data reduction pipeline. A standard set of ePESSTO+ OBs for calibrations and science is available on the ePESSTO+ wiki and the following sections describe how they are applied in the pipeline reduction process. An example of a fully calibrated SOFI spectrum (although observed during PESSTO and hence precedent to ePESSTO+ due to the paucity of NIR spectra) illustrating the wavelength range and atmospheric windows is shown in Fig. 1.

Bias, dark and cross-talk correction: the detector bias offset and structure is subtracted along with the sky background, as is standard procedure with his chip. The SOFI detector suffers from cross talk, where a bright source on either of the two upper or lower quadrants of the detector will be accompanied by a "ghost" on the corresponding row on the opposite two quadrants. This cross-talk effect is corrected for within the PESSTO pipeline by summing each row on the detector, scaling by a constant value, and subtracting from the opposite quadrants.

Flat field calibration: The lamp-off flats are subtracted from the lamp-on flats, to remove the thermal background of the system. These subtracted flat fields are combined and normalized and used to correct for the pixel-to-pixel variations in detector sensitivity in the science and standard star frames. The amplitude of the variability in the flat field is ~4% for the red grism and ~6% for the blue grism. Two normalized red grism flat fields taken ~5 months apart show exactly the same structure, demonstrating that the flat field is stable, and that the use of monthly calibrations is justified (see Smartt et al. 2015).

Arc frames and wavelength calibrations: wavelength calibration is performed using spectra of a Xenon arc lamp. To fit the dispersion solution of the arc spectra without any systematic residuals requires a 4th-order polynomial fit (see Table 2 for details of numbers of lines and RMS). This dispersion solution is applied to the two dimensional spectra and the sky lines are cross-correlated with an accurately calibrated template sky. A linear shift is applied to the wavelength calibration and recorded in the header keyword SHIFT. As with the EFOSC2 correction, the precision of the wavelength correction is limited to 0.1 Å, due to the scale of the shifts in the library sky spectra employed. Hence this value of 0.1 Å, is again recorded as the systematic error in the wavelength calibration (SPEC_SYE). As with EFOSC2 spectra, for all SOFI spectra the wavelength axis reports wavelengths as measured in dry air.

Sky subtraction and spectral extraction: SOFI spectra for PESSTO are taken in an ABBA dither pattern. This pattern consists of taking a first (A 1) exposure at position 'A', then moving the telescope so that the target is shifted along the slit of SOFI by ~5- 10'' to position 'B'. Two exposures are taken at 'B' (B1 and B2), before the telescope is offset back to 'A' where a final exposure (A2) is taken. The pipeline subtracts each pair of observations (i.e, A1 – B1, B1 – A1, B2 – A2, A2 – B2) to give individual bias- and sky-subtracted frames and shifts these sky-subtracted frames so that the trace of the target is at a constant pixel position, and the frames are then combined. Finally, the spectrum is optimally extracted interactively.

Telluric absorption correction: a "telluric standard" is observed immediately prior to or following the science spectrum, and at a similar airmass. The spectrum of the telluric standard is then divided by an appropriate template spectrum of the same spectral type, yielding an absorption spectrum for the telluric features. The absorption spectrum is then divided into the science spectrum to correct for the telluric absorption. As part of ePESSTO+, we observe either a Vega-like (spectral type A0V) or a Solar analogue (G2V) telluric standard for each SOFI spectrum. The PESSTO pipeline uses the closest (in time) observed telluric standard to each science or standard star spectrum

Spectrophotometric standards and flux calibration: the process for correcting the spectrum for the telluric absorption also provides a means for flux calibration using the Hipparcos I or V photometry of the solar analogs and Vega standards used. The flux of the observed telluric standard spectrum is scaled to match the tabulated photometry, with the assumption that the telluric standards have the same color (temperature) as Vega or the Sun. A second step is performed to flux calibrate the spectra using a spectrophotometric standard. The spectrophotometric standard is reduced and corrected for telluric absorption using a telluric standard, with the same technique as used for the

science targets. This corrected standard spectrum is then compared with its tabulated flux, and the science frame is then linearly scaled in flux to correct for any flux discrepancy. There are only a handful of spectrophotometric standard stars which have tabulated fluxes extending out as far as the K-band (listed in Table 2 of Smartt et al. 2015). All SOFI spectra have the following keyword which denotes which telluric standard was used for both the telluric correction and the initial flux calibration.

SENSFUN = 'Hip105672_20130816_GB_merge_57000_1_ex.fits' /tell stand frame

The spectrophotometric flux standard from Smartt et al. (2015; Table 3) used to additionally scale the flux and the keyword SENSPHOT is added to the header, with the spectrum used to apply the flux calibration. This file has the name of the standard labelled.

SENSPHOT= 'sens_Feige110_20130816_GB_merge_57000_1_f.fits' / sens used to flux cal

To improve the scaling of the absolute flux levels of the spectra, we employ the JHKs imaging that is normally done when SOFI spectra are taken. Synthetic J and H-band photometry was performed on the blue grism spectra, and H and K-band photometry on the red grism spectra. The magnitude offsets between the JHK synthetic photometry and the JHK aperture photometry provide scaling factors of the absolute flux levels applied to the spectra. We use the RMS of the zeropoints measured over the year as the typical uncertainty in the absolute flux calibration. This uncertainty in the absolute flux calibration is recorded in the headers of all SOFI spectra with the following header keyword (as done for EFOSC2) :

FLUXERR = 22.0 /Fractional uncertainty of the flux [%]

3. SOFI Near Infrared imaging

Bias, cross-talk and flat calibration: SOFI imaging is carried out as default when spectroscopy is done, providing images with a 4.9 arcmin field of view (0.29 arcsec pix^{-1}). The cross-talk effect is first corrected as for the spectra, and then all images are flat fielded using dome flats, which are typically taken on an annual basis. Pairs of flats are taken with the dome screen illuminated and un-illuminated; the latter are then subtracted from the former to account for bias and thermal background. Multiple flats are combined, and then used to reduce the science data. An illumination correction is also applied, to account for the difference between the illumination pattern of the dome flats and the actual illumination of the night sky. The illumination correction is determined by imaging a bright star at each position in a 4×4 grid on the detector. The intensity of the star is then measured at each position, and a two-dimensional polynomial is fitted. This polynomial is normalised to unity, so that it can be applied to the imaging data as a multiplicative correction.

Sky subtraction: For targets that are in relatively uncrowded fields, a dither pattern is employed where the telescope is moved to four offset positions on the sky, while keeping the target in the field of view ("on-source sky subtraction"). To determine the sky background, the four frames are then median combined without applying offsets, rejecting pixels from any individual image which are more than a certain threshold above the median. This initial sky image is subtracted from each individual frame in order to obtain initial sky-subtracted images. These frames are used to identify the positions of all sources and create a mask frame for each science image. For each set of four images, the frames are then median combined again without applying offsets and using the masks created previously to reject all sources and produce the final sky image. The final sky background image is then subtracted from each of the input frames. The sky-subtracted images are then mosaiced together to create a single image using the swarp package (Bertin et al. 2002). For targets which are in a crowded field, or where there is extended diffuse emission (such as nearby galaxies), ePESSTO+ observations alternate between observing the target, and observing an uncrowded off-source field around ~5 arcmin from the target (typically four frames on source, then four frames off source are observed, dithering in each case). The off-source frames are then used to compute a sky frame in the same way as for the "on-source sky subtraction". The off-source sky frame is then subtracted from each of the on-source images of the target, which are then combined to create the final image. Since the field of view of SOFI is rather small (4.9 arcmin) the astrometry is not set for

single images. Instead, sextractor is run to detect sources in individual frames, and to check the nominal dither.

Astrometric calibration: the astrometric calibration was derived using the 2MASS reference catalogues, and a distortion model described by a second-order polynomial. A typical scatter of 0.4-0.5 arcsec was been found for the science frames with around 15 stars usually recognised by the catalogue in the frame. This typically improves to an rms ~0.2-0.3 with ≳30 stars. The information on the RMS of RA and DEC is provided in the standard CRDER1 and CRDER2 keywords and repeated, along with the number of stars used for the calibration, in the ePESSTO+ specific keyword ASTROMET.

Photometric calibration: The individual SOFI images, which themselves are the result of the average combination of NDIT images, are then mosaiced together in a median combine using swarp., An astrometric calibration is made, by cross correlating the sources detected by sextractor with the 2MASS catalogue. The instrumental aperture magnitudes of the sources in the field as measured by daophot are then compared to their catalogued 2MASS magnitudes to determine the photometric zeropoint, which is recorded in the header of the image as PHOTZP without any further colour correction. The other relevant photometric keywords are as follows (see Smartt et al., 2015 for more details).

PSF_FWHM= 1.015714368/Spatial resolution (arcsec)
ELLIPTIC= 0.142 /Average ellipticity of point sources
PHOTZP = 25.4895217391 / MAG=-2.5*log(data)+PHOTZP
PHOTZPER= 0.09695742781/error in PHOTZP
FLUXCAL = 'ABSOLUTE' /Certifies the validity of PHOTZP
PHOTSYS = 'VEGA ' / Photometric system VEGA or AB
ABMAGSAT= 11.94145459901092/Saturation limit for point sources (AB mags)
ABMAGLIM= 18.96704572844871/ 5-sigma limiting AB magnitude for point sources

The zeropoint conforms to ESO SDP standards for archive images and can be employed simply as:

$$MAG = -2.5 \log(COUNTS\_ADU) + PHOTZP$$

where COUNTSADU is the measured signal in ADU. Users should be aware that these zeropoints are for guidance rather than for immediate and unchecked scientific use for photometry of transients. The zeropoints should always be checked with 2MASS sources, since the number and brightness of targets in automated selection various considerably due to the limited field of view of SOFI.

SOFI artifacts and problem images: the SOFI images are characterized by a number of recurring features which are mostly related to the sky subtraction method employed above. For example, Fig 2 shows an example image and its weight to illustrate the "on-source sky subtraction". The reader is referred to the PESSTO SSDR4 for further details.

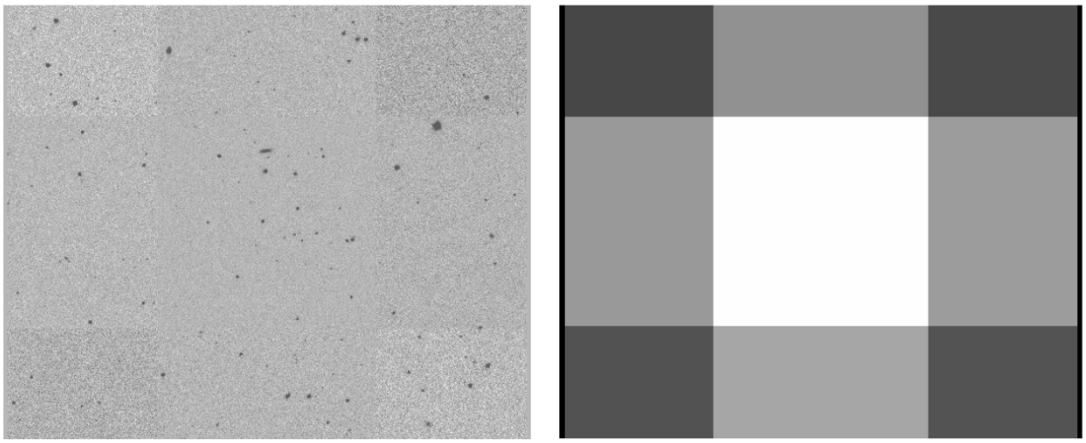

Figure 2. *The typical SOFI dither pattern for "on-source sky subtraction". The left panel shows a typical image, with the sky noise levels varying due to the dither pattern illustrated. The right panel is the weight image.*

Previous Releases

No previous releases

Data Format

EFOSC2 data file types and naming

One-dimensional flux calibrated spectra are in binary table format and conform to the ESO Science Data Products Standard (Retzlaff et al. 2013). The binary table FITS file consists of one primary header (there is no data in the primary HDU so NAXIS=0), and a single extension containing a header unit and a BINTABLE with NAXIS=2. A unique FITS file is provided for each individual science spectrum. The actual spectral data is stored within the table as vector arrays in single cells. As a consequence, there is only one row in the BINTABLE, that is NAXIS2=1. Information associated with the science spectrum is also provided within the same binary table FITS file resulting in a table containing one row with four data cells. The first cell contains the wavelength array in angstroms. The other three cells contain the science spectrum flux array (extracted with variance weighting), its error array (the standard deviation produced during the extraction procedure) and finally the sky background flux array. Each flux array is in units of erg cm^{-2} s^{-1} $Å^{-1}$. The science spectrum has a filename of the following form, prefix 't', object name, date of observation, grism, filter, slit width, MJD of data reduction date, a numeric counter (beginning at 1) to distinguish multiple exposures taken on the same night, and a suffix 'e' to denote a spectrum in binary table format.

tAT2021lm_20210107_Gr13_Free_slit1.0_59742_1_e.fits

In the few cases where the object name is longer than 20 characters, it is truncated within the filename to ensure the filename does not exceed the 68 characters limit enforced by ESO. The full object name is always recorded in the OBJECT keyword. They can be identified as having the data product category keyword set as

PRODCATG = SCIENCE.SPECTRUM /Data product category

The 2D spectrum images which can be used to re-extract the object as discussed above are released as associated ancillary data. They are associated with the science spectra through the following header keywords in the science spectra files. The file name is the same as for the 1D spectrum, but the suffix used '2df' to denote an image.

ASSON1 = tAT2021lm_20210107_Gr13_Free_slit1.0_59742_1_2df.fits /Name of associated file

These 2D files are wavelength and flux calibrated hence a user can re-extract a region of the data and have a calibrated spectrum immediately. Users should note the value for BUNIT in these frames means that the flux should be divided by 10^{20} to provide the result in erg cm^{-2} s^{-1} Å-1.

SOFI data file types and naming

The data products for SOFI are similar to those described above for EFOSC2. The spectra are in binary table FITS format, with the same four data cells corresponding to the wavelength in angstroms, the weighted science spectrum and its error and the sky background flux array. Again, each flux array is in units of erg cm^{-2} s^{-1} $Å^{-1}$. The SSDR1 FITS keywords described Smartt et al. (2015) are again applicable here. A typical file name is

SN2021yja_20210924_GR_merge_59669_1_sc.fits

Where the object name is followed by the date observed, the grism (GB for the blue grism, or GR for the red grism), the word "merge" to note that that the individual exposures in the ABBA dither pattern have been co-added, the date the file was created, a numeric value to distinguish multiple exposures on the same night and the suffix 'sc' to refer to a science object. As with EFOSC2, this science spectrum can be identified with the label:

PRODCATG = SCIENCE.SPECTRUM /Data product category

We also provide the 2D flux calibrated and wavelength calibrated file so that users can re-extract their object directly, as described with EFOSC2. The identification of the 2D images follows the same convention as for EFOSC2, with the suffix '2df' to denote a spectral image.

ASSON1 = SN2021yja_20210924_GR_merge_59669_1_2df.fits /Name of associated file

In nearly all cases where PESSTO takes a SOFI spectrum, imaging in JHKs is also taken. These images are flux and astrometrically calibrated and released as science frames. They are labeled as follows where Ks labels the filter and the merge denotes that the dithers have been median combined.

SN2019cxx_20190501_Ks_merge_59669_1.fits

We also release the image weight map as described in (Retzlaff et al. 2013). The definition in this document is the pixel-to-pixel variation of the statistical significance of the image array in terms of a number that is proportional to the inverse variance of the background, i.e. not including the Poisson noise of sources. This is labelled as

ASSON1 = SN2019cxx_20190501_Ks_merge_59669_1.weight.fits /Name of associated file

Catalogue Columns

This release does not provide an ePESSTO+ Transient Catalogue.

Acknowledgements

Any publication making use of this data, whether obtained from the ESO archive or via third parties, must include the following acknowledgment:

Smartt S.J. et al. 2015, A&A, 579, 40: PESSTO: survey description and products from the first data release of the Public ESO Spectroscopic Survey of Transient Objects

And please also add the following acknowledging statement in your articles Based on data products from observations made with ESO Telescopes at the La Silla Paranal Observatory under programmes 1103.D-0328 and 106.216C: ePESSTO+ (the advanced Public ESO Spectroscopic Survey for Transient Objects).

References

Moran, S., Fraser, M., Kotak, R., et al. (2023) "A long life of excess: The interacting transient SN 2017hcc," A&A, 669, A51 - 2023A&A...669A..51M

Onori, F., Cannizzaro, G., Jonker, P. G., et al. (2022) "The nuclear transient AT 2017gge: a tidal disruption event in a dusty and gas-rich environment and the awakening of a dormant SMBH," MNRAS, 517, 76-98 - 2022MNRAS.517...76O

Wevers, T., Nicholl, M., Guolo, M., et al. (2022) "An elliptical accretion disk following the tidal disruption event AT 2020zso," A&A, 666, A6 - 2022A&A...666A...6W

Hosseinzadeh, G., Kilpatrick, C. D., Dong, Y., et al. (2022) "Weak Mass Loss from the Red Supergiant Progenitor of the Type II SN 2021yja," ApJ, 935, 31 - 2022ApJ...935...31H

Medler, K., Mazzali, P. A., Teffs, J., et al. (2022) "SN 2020acat: an energetic fast rising Type IIb supernova," MNRAS, 513, 5540-5558 - 2022MNRAS.513.5540M

Irani, I., Prentice, S. J., Schulze, S., et al. (2022) "Less Than 1% of Core-collapse Supernovae in the Local Universe Occur in Elliptical Galaxies," ApJ, 927, 10 - 2022ApJ...927...10I

Charalampopoulos, P., Leloudas, G., Malesani, D. B., et al. (2022) "A detailed spectroscopic study of tidal disruption events," A&A, 659, A34 - 2022A&A...659A..34C

Perley, D. A., Ho, A. Y. Q., Yao, Y., et al. (2021) "Real-time discovery of AT2020xnd: a fast, luminous ultraviolet transient with minimal radioactive ejecta," MNRAS, 508, 5138-5147 - 2021MNRAS.508.5138P

Prentice, S. J., Inserra, C., Schulze, S., et al. (2021) "Transitional events in the spectrophotometric regime between stripped envelope and superluminous supernovae," MNRAS, 508, 4342-4358 - 2021MNRAS.508.4342P

Parrag, E., Inserra, C., Schulze, S., et al. (2021) "SN 2019hcc: a Type II supernova displaying early O II lines," MNRAS, 506, 4819-4840 - 2021MNRAS.506.4819P

Medler, K., Mazzali, P. A., Teffs, J., et al. (2021) "SN 2020cpg: an energetic link between Type IIb and Ib supernovae," MNRAS, 506, 1832-1849 - 2021MNRAS.506.1832M

Cannizzaro, G., Wevers, T., Jonker, P. G., et al. (2021) "Accretion disc cooling and narrow absorption lines in the tidal disruption event AT 2019dsg," MNRAS, 504, 792-815 - 2021MNRAS.504..792C

Barna, B., Szalai, T., Jha, S. W., et al. (2021) "SN 2019muj - a well-observed Type Iax supernova that bridges the luminosity gap of the class," MNRAS, 501, 1078-1099 - 2021MNRAS.501.1078B

Gutiérrez, C. P., Pastorello, A., Jerkstrand, A., et al. (2020) "SN 2017ivv: two years of evolution of a transitional Type II supernova," MNRAS, 499, 974-992 - 2020MNRAS.499..974G

Nicholl, M., Wevers, T., Oates, S. R., et al. (2020) "An outflow powers the optical rise of the nearby, fast-evolving tidal disruption event AT2019qiz," MNRAS, 499, 482-504 - 2020MNRAS.499..482N

Short, P., Nicholl, M., Lawrence, A., et al. (2020) "The tidal disruption event AT 2018hyz - I. Double-peaked emission lines and a flat Balmer decrement," MNRAS, 498, 4119-4133 - 2020MNRAS.498.4119S

Leloudas, G., Dai, L., Arcavi, I., et al. (2019) "The Spectral Evolution of AT 2018dyb and the Presence of Metal Lines in Tidal Disruption Events," ApJ, 887, 218 - 2019ApJ...887..218L

Smartt, S. J., Valenti, S., Fraser, M., et al. (2015) "PESSTO: survey description and products from the first data release by the Public ESO Spectroscopic Survey of Transient Objects," A&A, 579, A40 - 2015A&A...579A..40S